Optical and Thermal Sensing for Additive Manufacturing

Albert C. To, Ph.D.
William Kepler Whiteford Professor
with contributions from Shawn Hinnebusch, Berkay Bostan, David Anderson, Alaa Olleak, Xuan Liang, Ran Zou (ECE Dept.), Prof. Kevin Chen (ECE Dept.)
Department of Mechanical Engineering and Materials Science
University of Pittsburgh

Virtual Workshop on Optical Sensors for Energy Applications
March 2, 2023

ANSYS ADDITIVE MANUFACTURING RESEARCH LABORATORY

Ansys Additive Manufacturing Research Lab (AMRL)

- Established in 2015
- 2,000 sq ft lab space

Optomec LENS 450

EOS M290 DMLS

ExOne Innovent

GEFERTEC arc605

AM Build Failures

EOS M290 DMLS

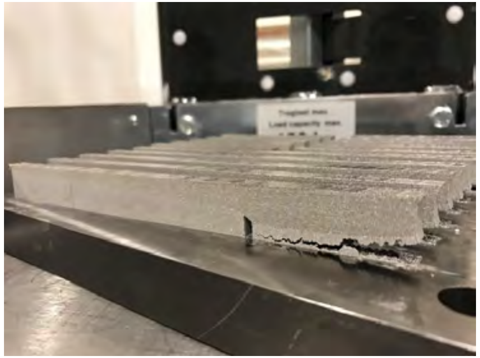

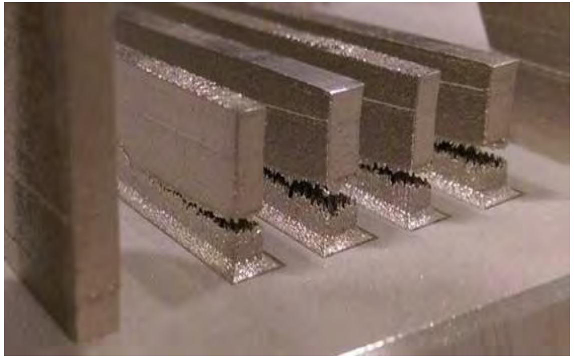

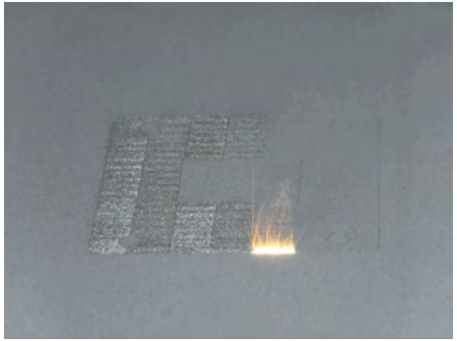

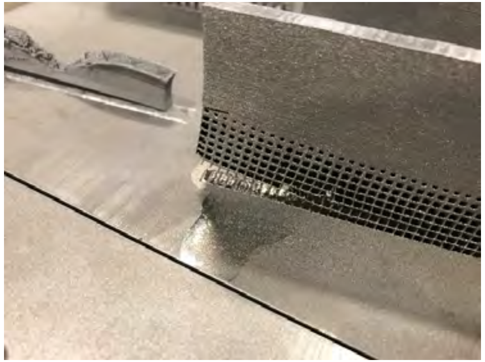

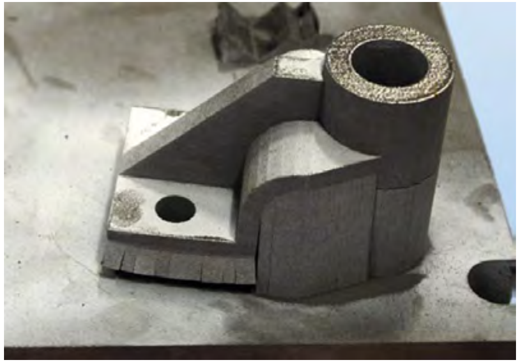

PITT | SWANSON ENGINEERING
ANSYS ADDITIVE MANUFACTURING RESEARCH LABORATORY

Efficient Residual Stress Modeling

Detailed model
- Meso-scale (~0.1mm)
- Sequentially coupled thermomechanical analysis

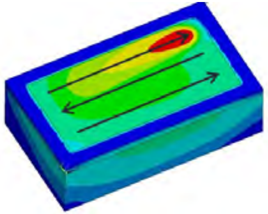

Extract inherent strains (element-by-element)

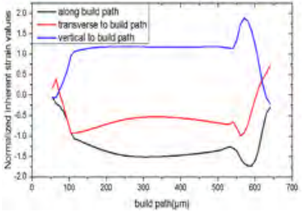

$$\varepsilon^{In} = \varepsilon_{t_i}^{Plastic} + (\varepsilon_{t_i}^{Elastic} - \varepsilon_{t_s}^{Elastic})$$

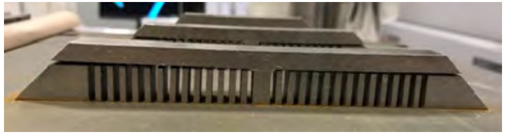

After cutting

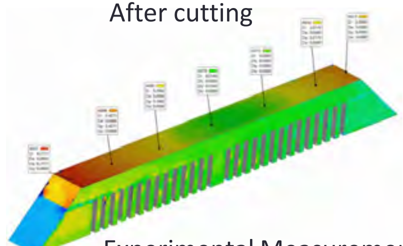

Experimental Measurement

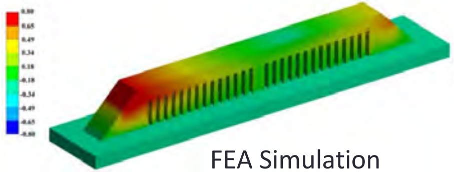

FEA Simulation

Inherent strain model
- Macro-scale (~100mm)
- Quasi-static mechanical analysis

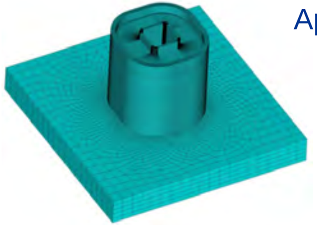

Apply inherent strains (layer-by-layer)

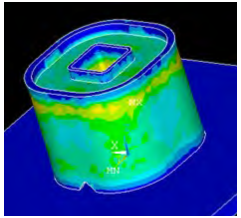

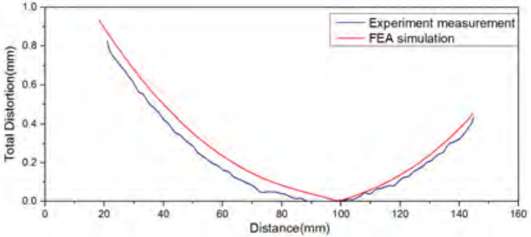

➢ **Reduce error in deformation from 40% to 10% compared to original inherent strain model**

Q. Chen, **A. C. To**, et al., "An inherent strain based multiscale modeling framework for simulating part-scale residual deformation for direct metal laser sintering," *Additive Manufacturing*, vol. 28, 406-418, 2019.
X. Liang, **A. C. To**, et al., "Modified inherent strain method for fast prediction of residual deformation in direct metal laser sintered components," *Computational Mechanics*, vol. 64, 1719-1733, 2019.

Thermal Model Calibration

Goldak heat source model: $Q = \frac{6\sqrt{3}P\eta}{abc\pi\sqrt{\pi}} exp\left(-\frac{3(x_0 + vst - x')^2}{a^2} - \frac{3(y' - y_0)^2}{b^2} - \frac{3(z' - z_0)^2}{c^2}\right)$

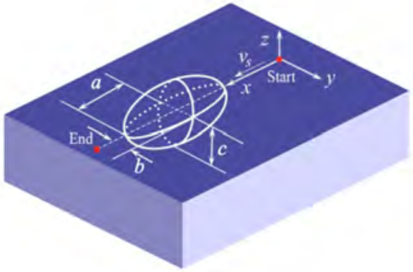

laser power: *P*
laser absorptivity: η
local coordinates : x', y', z'
Geometric factors: a, b, c

J. Goldak, A. Chakravarti, M. Bibby, Metall. Trans. B 15B (1984) 299-305

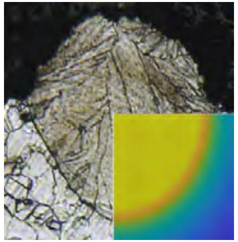

Melt pool cross section

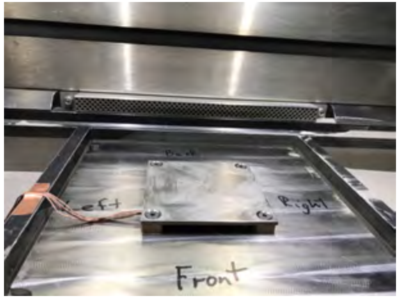

In-situ thermocouples

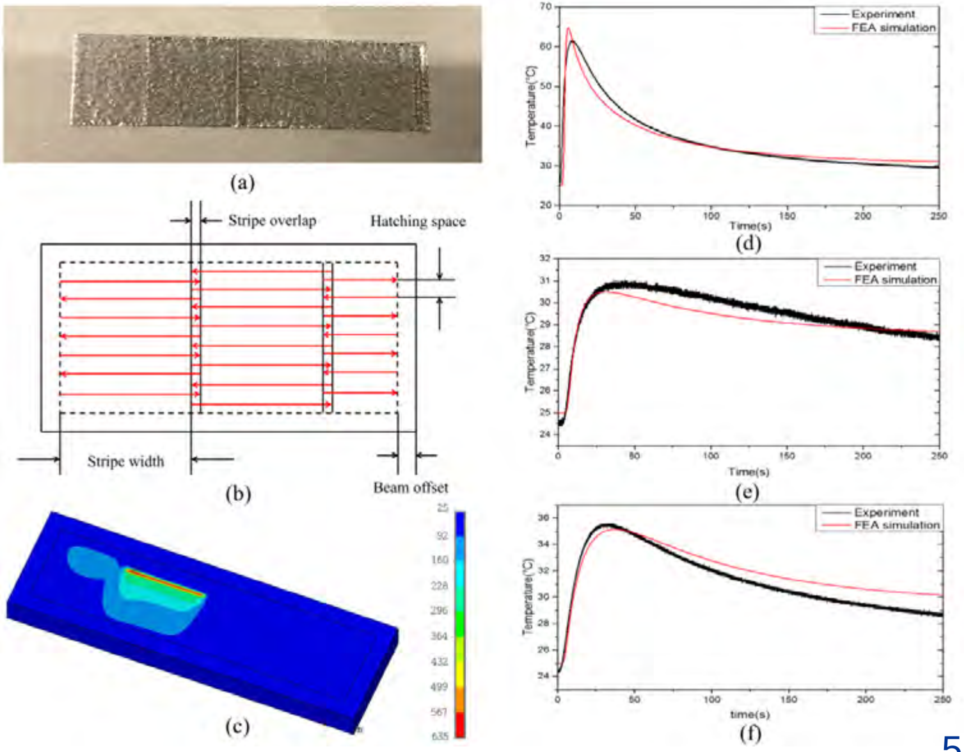

PITT SWANSON ENGINEERING
ANSYS ADDITIVE MANUFACTURING RESEARCH LABORATORY

Sensor-Fused AM Process

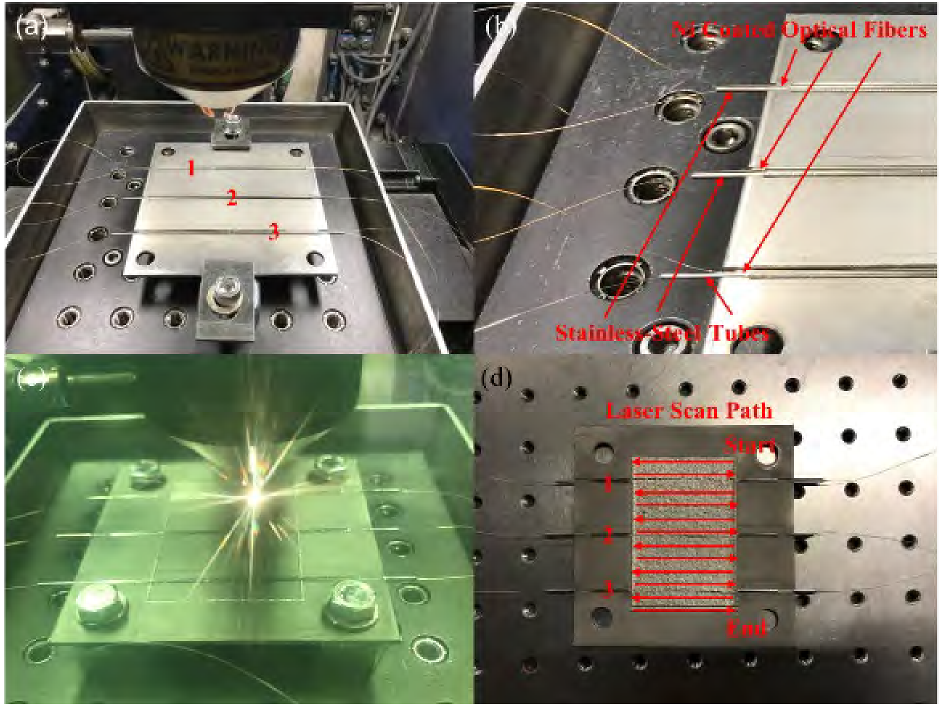

Sensor Fused AM Process

- High resolution real-time T & με measurements
- Design proper structures to embed sensors without disturbing AM process and part itself
- Real-time measurements to study AM process itself
- Post-process monitoring to study residual strain formation and relaxation.
- Compare, correct, and validate DT

PITT | SWANSON ENGINEERING
ANSYS ADDITIVE MANUFACTURING RESEARCH LABORATORY

R. Zou, X. Liang, A. C. To, K. P. Chen, et al., A Digital Twin Approach to Study Additive Manufacturing Processing Using Embedded Optical Fiber Sensors and Numerical Modeling. IEEE Journal of Lightwave Technology, 6402-6411, 2020.

Sensor-Fused AM Process

(a) Detailed simulation

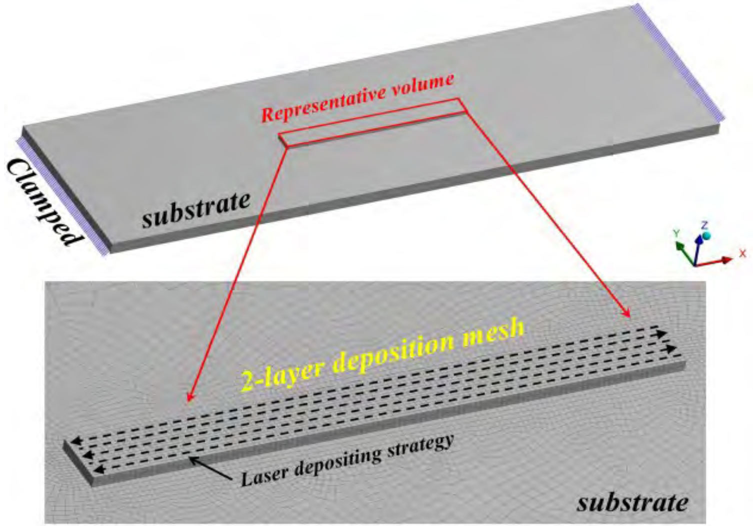

(b) Strain from simulation and experimental results

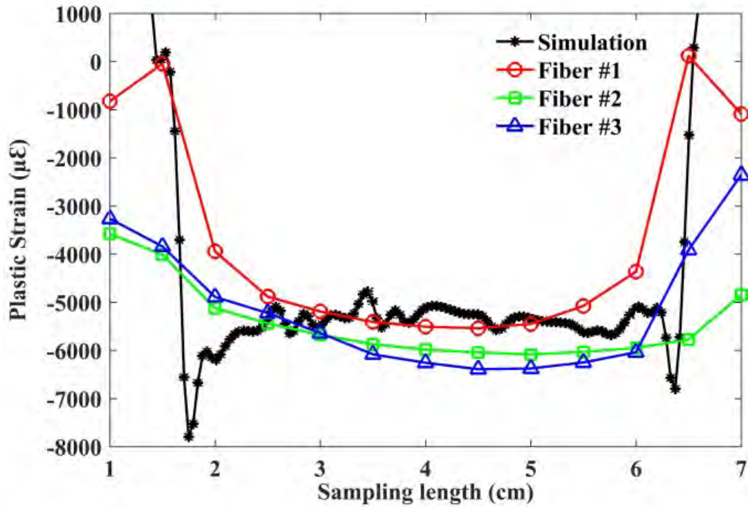

R. Zou, X. Liang, A. C. To, K. P. Chen, et al., A Digital Twin Approach to Study Additive Manufacturing Processing Using Embedded Optical Fiber Sensors and Numerical Modeling. IEEE Journal of Lightwave Technology, 6402-6411, 2020.

Defects in Laser Powder Bed AM

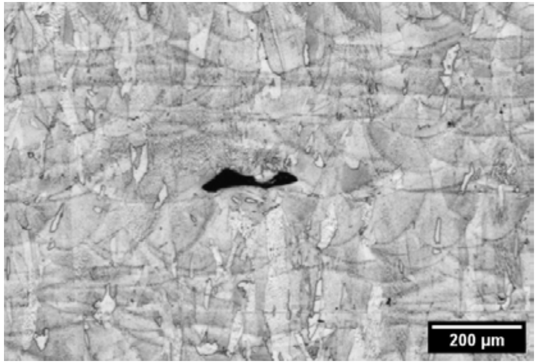

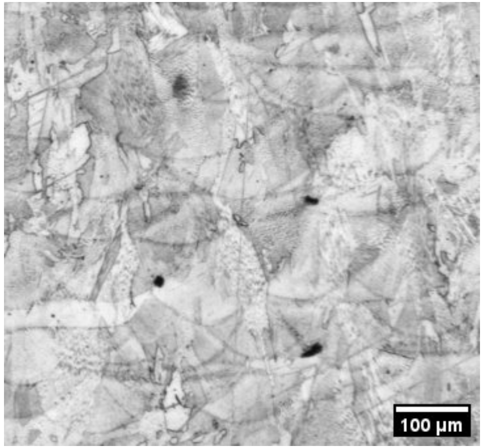

In-Situ Defect Detection Using IR Imaging and ML

Inputs
- Heat intensity
- Cooling rate
- Interpass temperature
- Local spatter counts

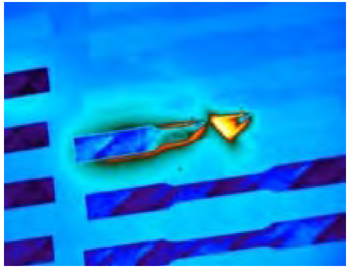

Deep Neural Networks

Outputs
- Local porosity
- Defect type
- Maximum defect size

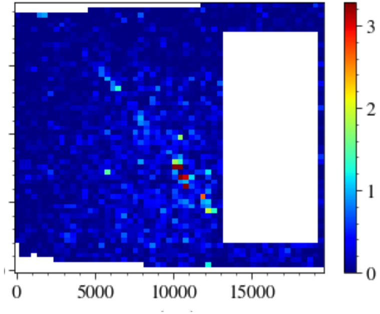

Infrared (IR) camera

Aims to estimate the defects in LBPF-manufactured parts from in-situ IR monitoring data using deep learning

In-Situ IR Camera

- The camera is mounted on an EOS M290 DMLS machine
- 640x480 Pixel detector
  - 360 µm pixel size
- Frame Rate: 30 (FPS)
- Ranges:
  - -20 – 120 °C
  - **0 – 650 °C**
  - 300 – 2,000 °C

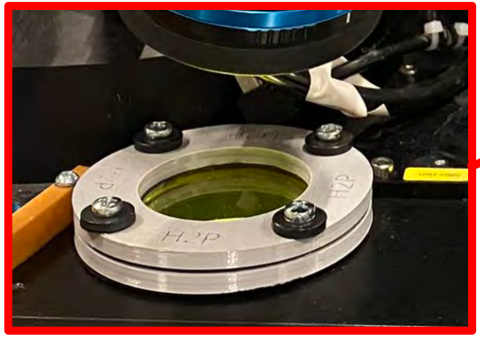

PITT | SWANSON ENGINEERING
ANSYS ADDITIVE MANUFACTURING RESEARCH LABORATORY

In-Situ IR Signature Extraction

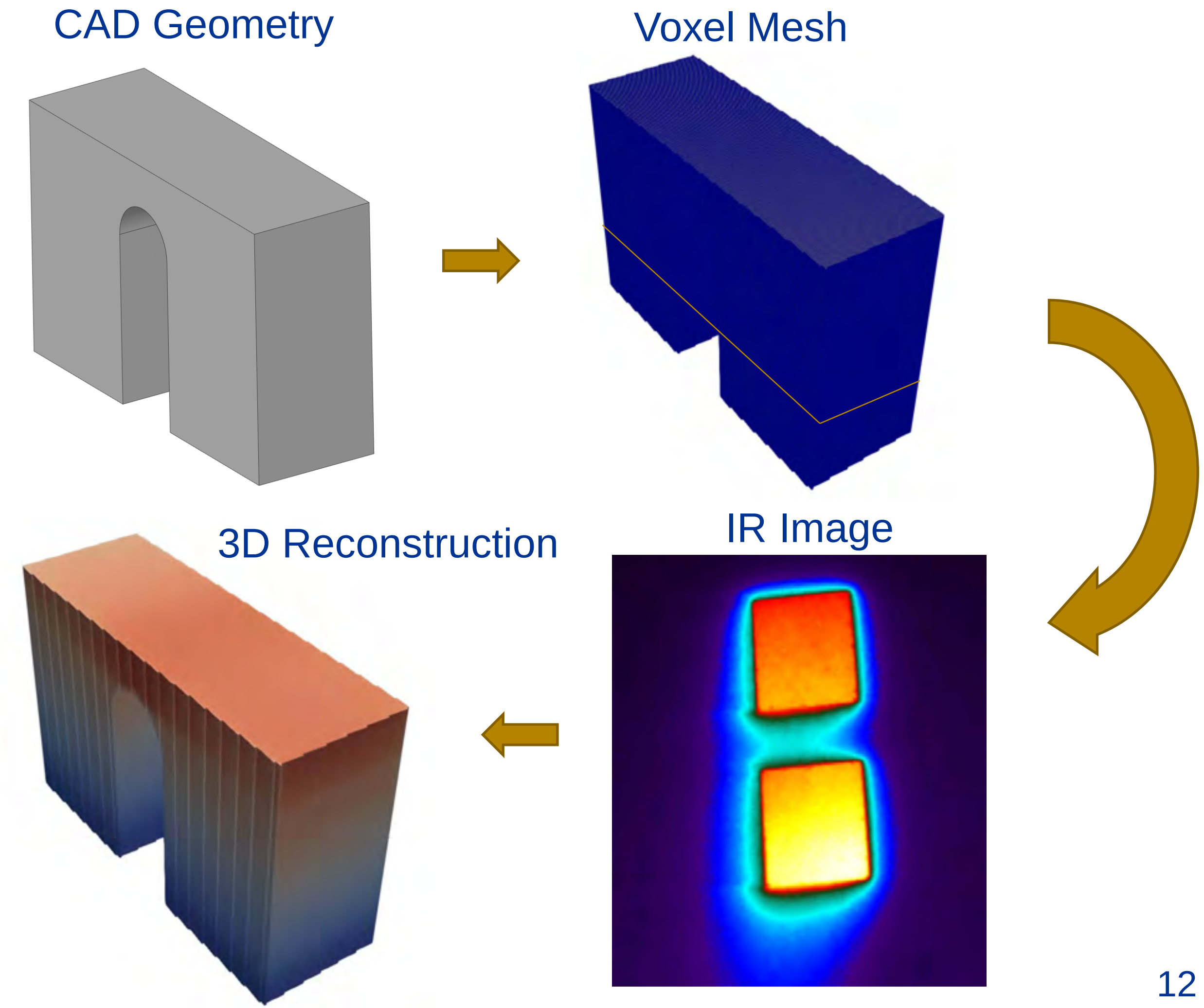

- Understand causal relationship with porosity
- Reduce data storage and enable real-time processing

PITT | SWANSON ENGINEERING
ANSYS ADDITIVE MANUFACTURING RESEARCH LABORATORY

Complex Part: Heat Map

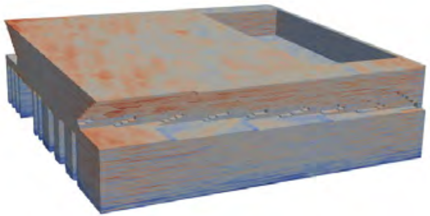

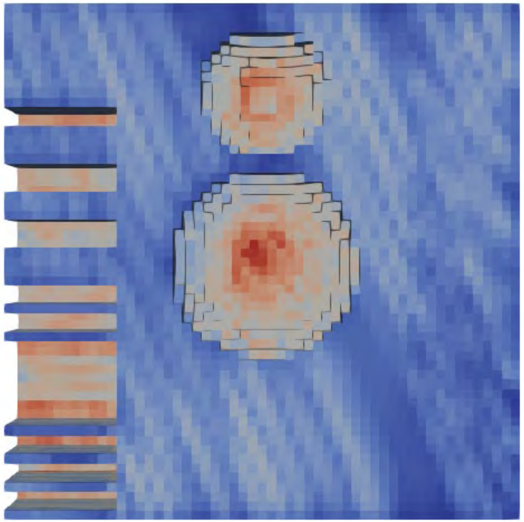

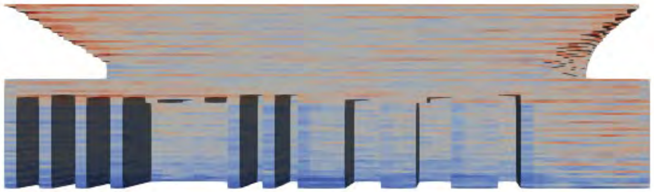

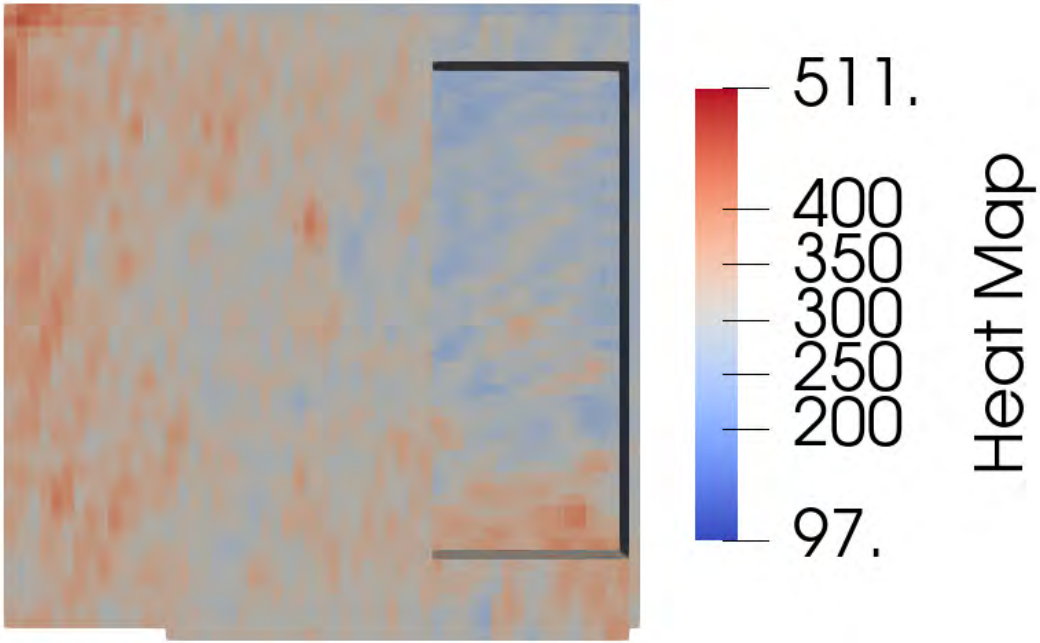

Complex Part: Interpass Temperature

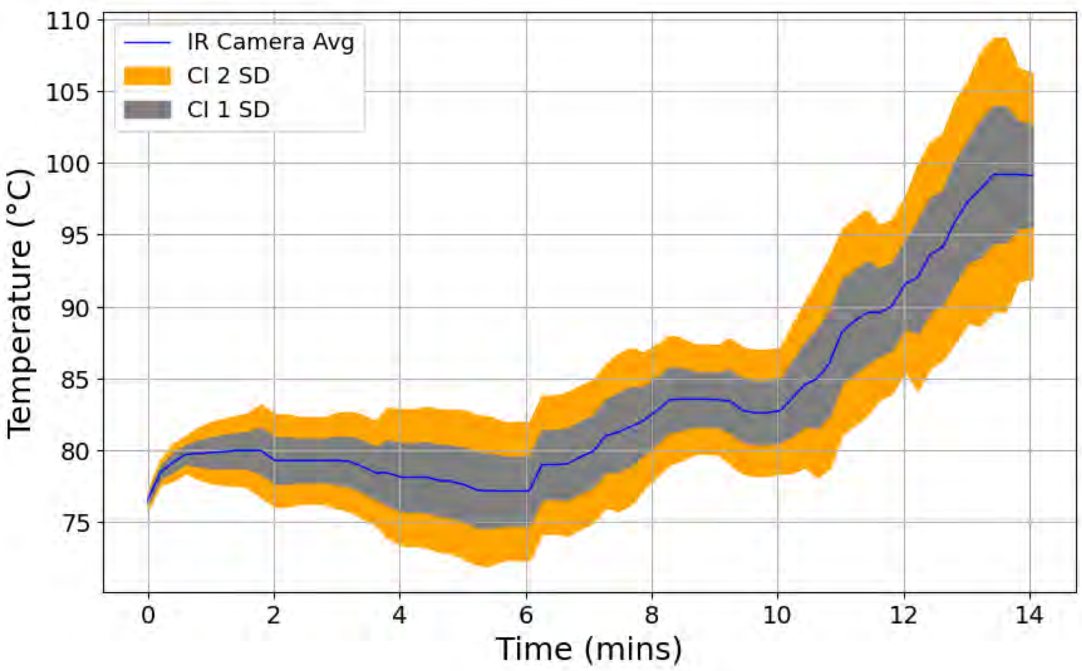

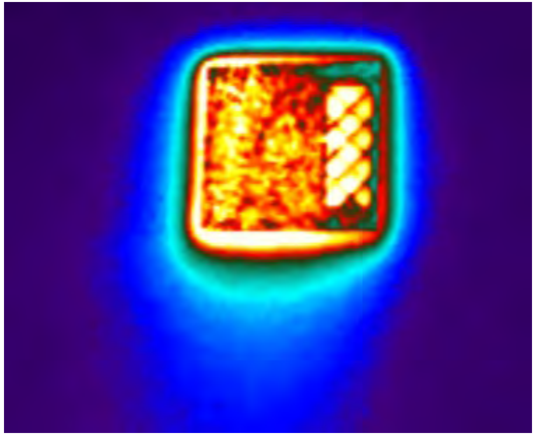

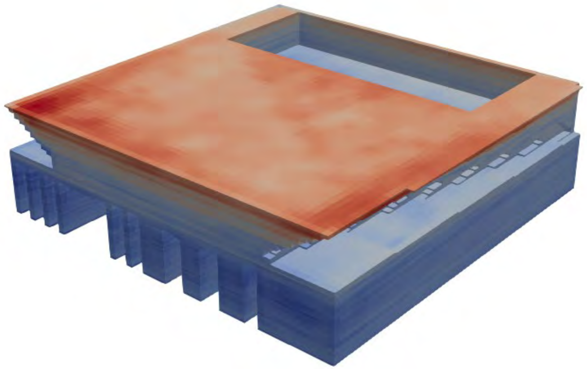

PITT | SWANSON ENGINEERING
ANSYS ADDITIVE MANUFACTURING RESEARCH LABORATORY

In-Situ IR Signatures

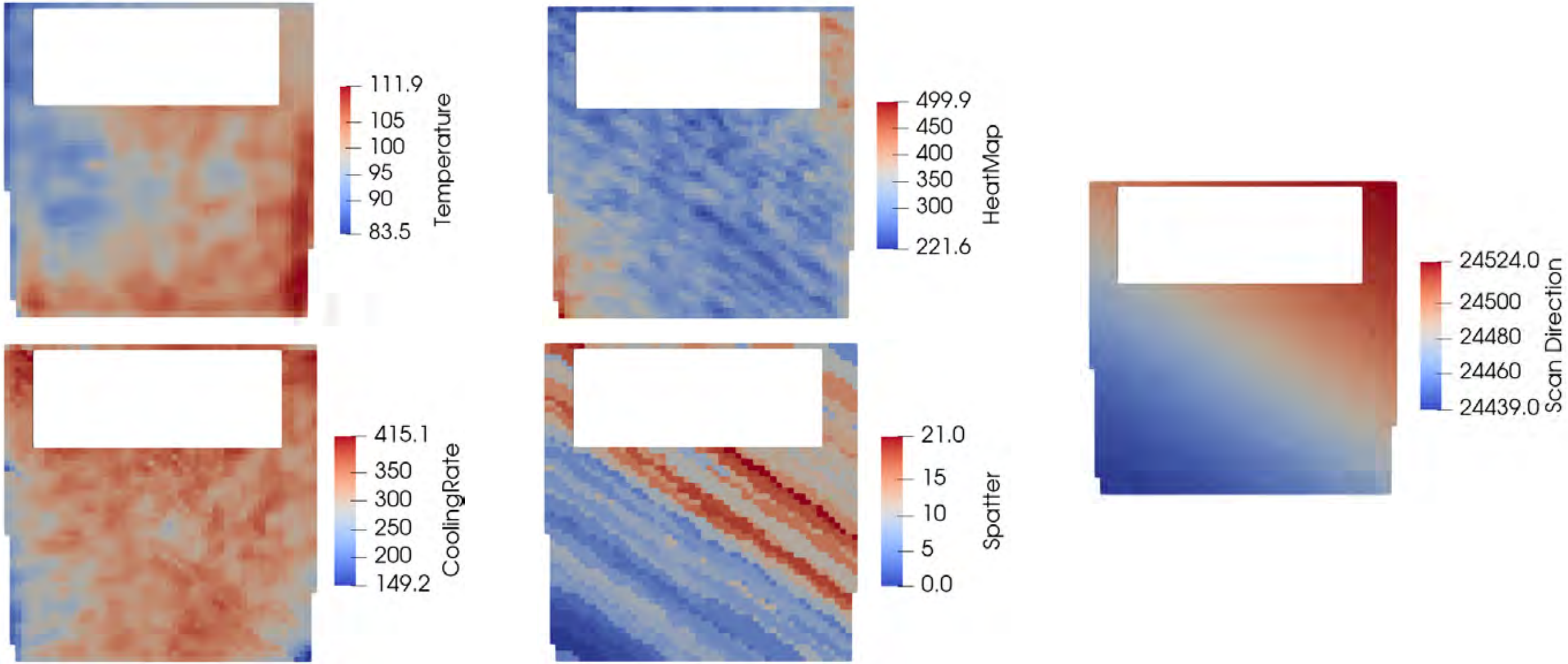

Porosity Analysis

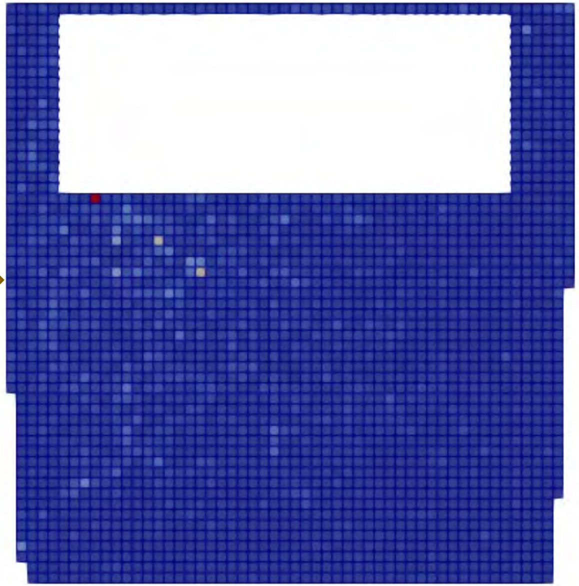

DNNs Porosity Prediction

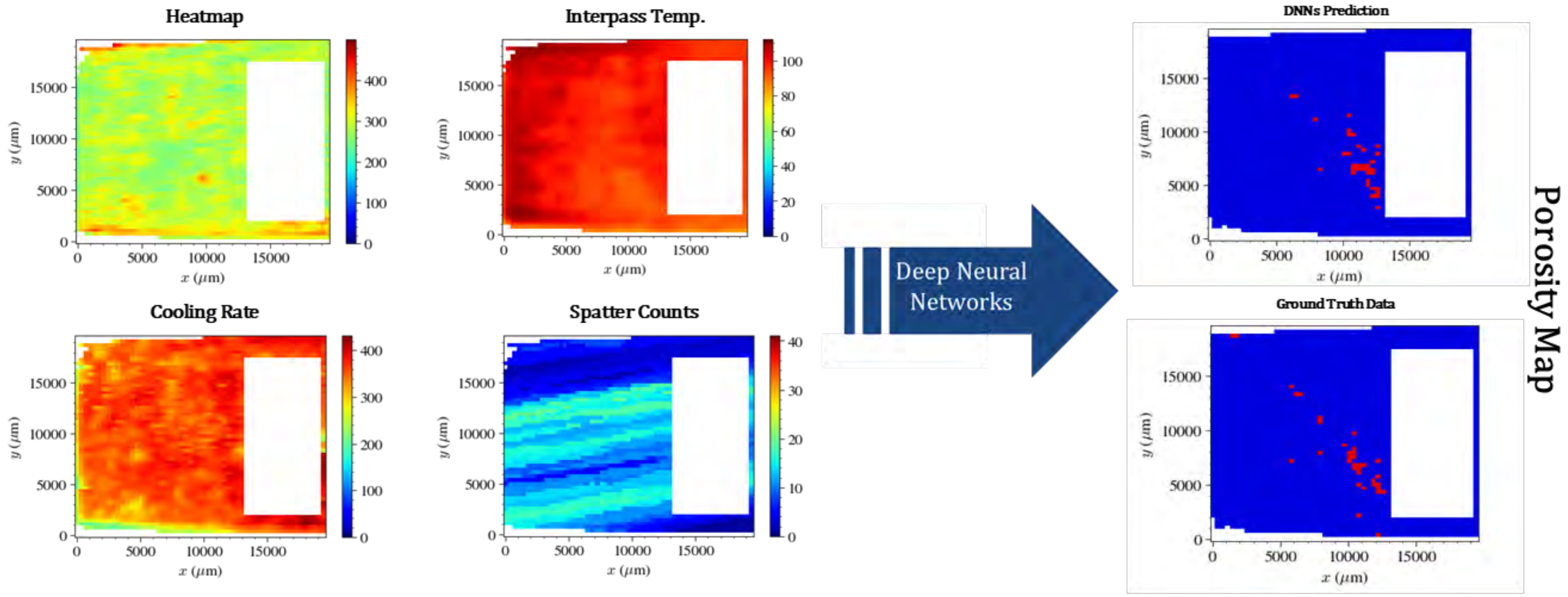

Prediction accuracy over 90% for porosity over 0.8% (~50 μm)

PITT | SWANSON ENGINEERING
ANSYS ADDITIVE MANUFACTURING RESEARCH LABORATORY

Feature Importance Analysis by SHAP (SHapley Additive exPlanations) Method

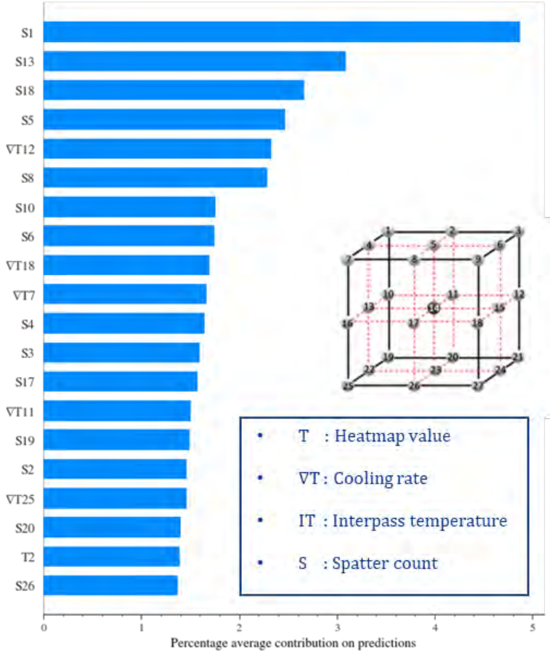

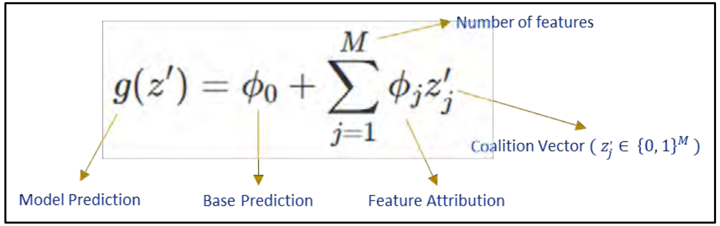

Analysis of a sample prediction

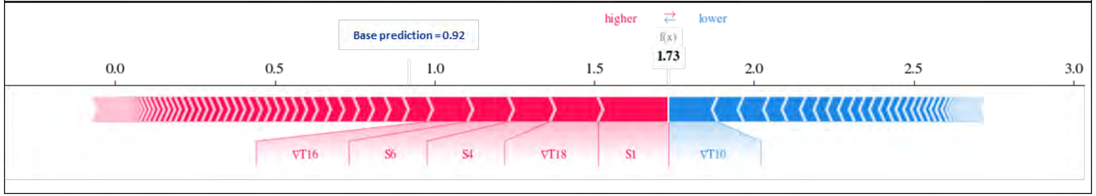

For more details: https://christophm.github.io/interpretable-ml-book/shap.html

PITT | SWANSON ENGINEERING
ANSYS ADDITIVE MANUFACTURING RESEARCH LABORATORY

Inverse Correlation between Spatter Counts and Porosity

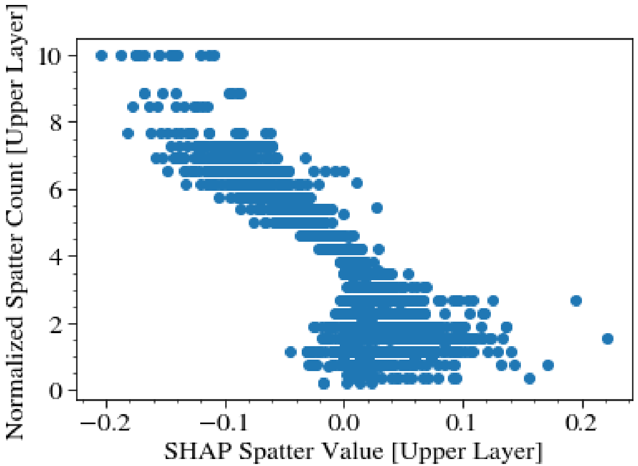

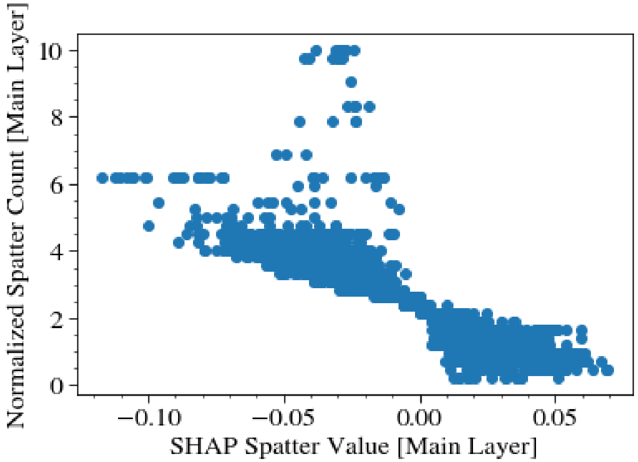

What About the Cooling Rate and Heatmap?

- Higher cooling rates cause more porosity

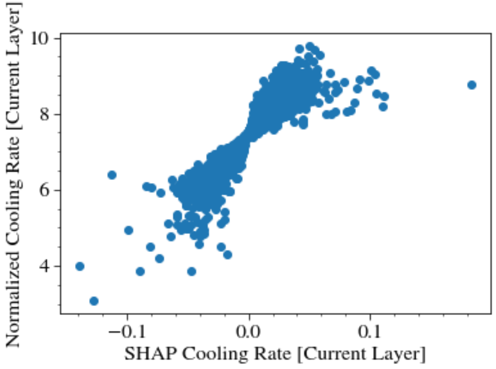

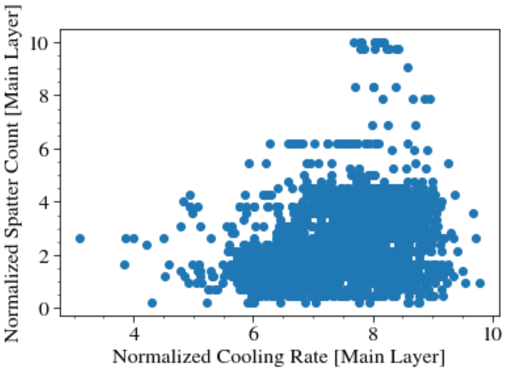

- correlation between spatter count and cooling rate not clear

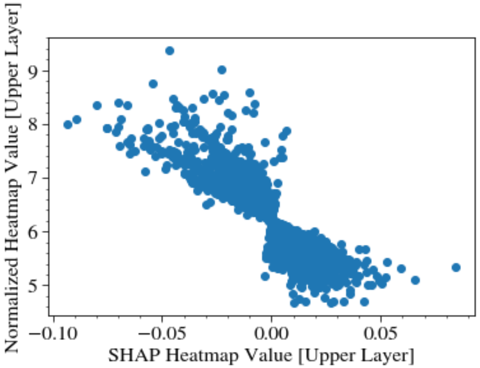

- Inverse correlation between maximum heat intensity and porosity

PITT | SWANSON ENGINEERING
ANSYS ADDITIVE MANUFACTURING RESEARCH LABORATORY

Conclusions

- Optical fiber successfully embedded using AM and deformation measurement validated
- Various key signatures can be extracted from a single IR camera for detecting defects
- Porosity predictor DNNs developed have more than 90% prediction accuracy for porosity greater than 0.8% (~50 µm)
- Possible defect generation mechanisms found:
    - Spatter generation is the most dominant feature of lof-pore generation
    - High cooling rates and low heat intensity cause lof-pore generation

Future Work

- Develop algorithms to obtain other key defect signatures
- Use simulation data to improve ML predictions
- Integrate optical fiber sensing into in-situ AM monitoring

Thank You!

- Prof. Albert C. To
- albertto@pitt.edu
- Department of Mechanical Engineering & Material Science
- University of Pittsburgh

?